Remote Sensing of Solar-Stimulated Phytoplankton Chlorophyll Fluorescence by Differential Absorption in the Oxygen B-band

Robert Frouin[a], Pierre-Yves Deschamps[b], Philippe Dubuisson[b]
[a]Scripps Institution of Oceanography University of California at San Diego,
9500 Gilman Drive, La Jolla, California 92093-0224
[b]Laboratoire d'Optique Atmosphérique, Université des Sciences et Technologies de Lille,
59655 Villeneuve d'Ascq, France

ABSTRACT

A new methodology is proposed to estimate from space the solar-induced chlorophyll fluorescence of natural waters. The methodology exploits absorption in the oxygen B-band around 687 nm, located near the peak of fluorescence emission at 685 nm. Inside the oxygen absorption lines, the fluorescence signal enhances the reflected solar radiance. By using a pair of spectral bands inside and outside the absorption region, or more generally spectral bands for which oxygen absorption is sufficiently different, the emitted contribution to the measured radiance can be extracted. Feasibility is demonstrated and retrieval accuracy quantified through simulations of the top-of-atmosphere reflectance by a radiation transfer code that fully accounts for multiple scattering and interactions between scattering and absorption. The differential absorption method works well from just above the surface. Pairs of spectral bands centered on the same wavelength provide the best results. Using spectral bands of 686.8-688.3 nm and 683.1-692.0 nm, the expected accuracy on fluorescence retrievals is <10% for chlorophyll concentrations above 1 mgm^{-3}. Performance is degraded from space, due to the influence of aerosol vertical structure on the oxygen transmittance associated with path reflectance. In this case, knowledge of aerosol reflectance and optical thickness is required, but assuming an average aerosol vertical distribution yields reasonable results. In comparison with the standard baseline technique, significant improvements in retrieval accuracy are expected in Case II waters, especially in the presence of sediments.

Key words: Remote sensing, phytoplankton, fluorescence, chlorophyll, ocean color, oxygen absorption, and aerosols

1. INTRODUCTION

The solar-induced chlorophyll fluorescence of natural waters depends on the incident irradiance, the light absorbed by phytoplankton, and the quantum yield of fluorescence. It is linked to phytoplankton abundance and activity. Fluorescence measurements provide information on chlorophyll concentration and the physiological state of phytoplankton. The quantum yield of fluorescence, influenced by phytoplankton type and environmental factors such as nutrient supply and light availability, may be used to discriminate species (e.g., harmful algae blooms) and to detect environmental stresses (e.g., Fe limitation). Despite the difficulty to interpret measurements, fluorescence is important to understanding the physiology of phytoplankton and investigating environmental influences on primary production and food web structure.

Remote Sensing of Inland, Coastal, and Oceanic Waters, edited by Robert J. Frouin,
Serge Andrefouet, Hiroshi Kawamura, Mervyn J. Lynch, Delu Pan, Trevor Platt,
Proc. of SPIE Vol. 7150, 715005 · © 2008 SPIE · CCC code: 0277-786X/08/$18 · doi: 10.1117/12.806386

Chlorophyll fluorescence can be measured remotely from above the surface[1], and it is now routinely observed from space by the MODIS and MERIS instruments[2]. The algorithms for estimating the fluorescence signal involve the subtraction of a baseline representing the shape of the water reflectance spectrum without fluorescence, i.e., the elastic contribution[3, 4]. Three spectral bands are typically used, centered at 665, 682, and 705 nm for MERIS and 665, 677, and 746 for MODIS. In waters containing sediments and yellow substances (Case II waters), determination of the baseline may not be accurate, yielding unacceptable uncertainties in the fluorescence estimates, all the more as the chlorophyll concentration or the quantum yield of fluorescence are low. It is desirable to improve accuracy in these waters, for which fluorescence, unlike blue-to-green reflectance ratios, is a good measure of chlorophyll concentration.

In this context, a new methodology is presented to estimate the fluorescence signal from natural waters. This methodology is based on differential absorption in the oxygen B-band centered on 687 nm. The oxygen absorption lines are partially filled due to inelastic fluorescence emission, which peaks at 685 nm for chlorophyll, and measuring the change with respect to reflected solar radiance (i.e., to the elastic component), yields a measure of the fluorescence signal. Note that many compounds found in yellow matter also fluoresce, but their effects are negligible above 600 nm, i.e., they do not interfere with chlorophyll fluorescence. The methodology is evaluated theoretically for measurements from just above the surface or from space. The effects of aerosol altitude and elastic water reflectance on the fluorescence estimation are investigated, allowing the selection of optimum spectral bands and the development of a suitable retrieval algorithm.

2. DIFFERENTIAL ABSORPTION TECHNIQUE USING OXYGEN B-BAND

In the B-band, oxygen absorption occurs between 685 and 695 nm (Figure 1). Water vapor absorption also exists in this spectral range, but is weak and can be neglected below 692 nm. Consider two spectral bands, one strongly affected by oxygen absorption, the other not, or minimally affected, by oxygen absorption. In the following these spectral bands will be denoted by superscripts (1) and (2), respectively. For clarity and simplification, it is assumed that oxygen absorption only occurs in the spectral band denoted by superscript (1). Furthermore, sun glint is neglected as well as Raman scattering. Two cases are investigated, the case of viewing the ocean from just above the surface and the case of viewing the ocean from space.

Measuring from just above the surface

Further neglecting sky light reflection by the surface, the radiance L_0 measured from just above the surface can be expressed as:

$$L_0^{(1)} = \rho_w^{(1)} E_s^{(1)} \cos(\theta_s) T_d^{(1)}(\theta_s) T_{O2}^{(1)}(\theta_s, P_0)/\pi + L_F^{(1)} \quad (1a)$$

$$L_0^{(2)} = \rho_w^{(2)} E_s^{(2)} \cos(\theta_s) T_d^{(2)}(\theta_s)/\pi + L_F^{(2)} \quad (1b)$$

where E_s is the extraterrestrial solar irradiance, T_d is the diffuse atmospheric transmittance for solar zenith angle θ_s, T_{O2} is the oxygen transmittance along the path sun to surface (pressure P_0), ρ_w is the elastic water reflectance, and L_F is the radiance due to chlorophyll fluorescence. Note that results would be similar if sky light reflection were included.

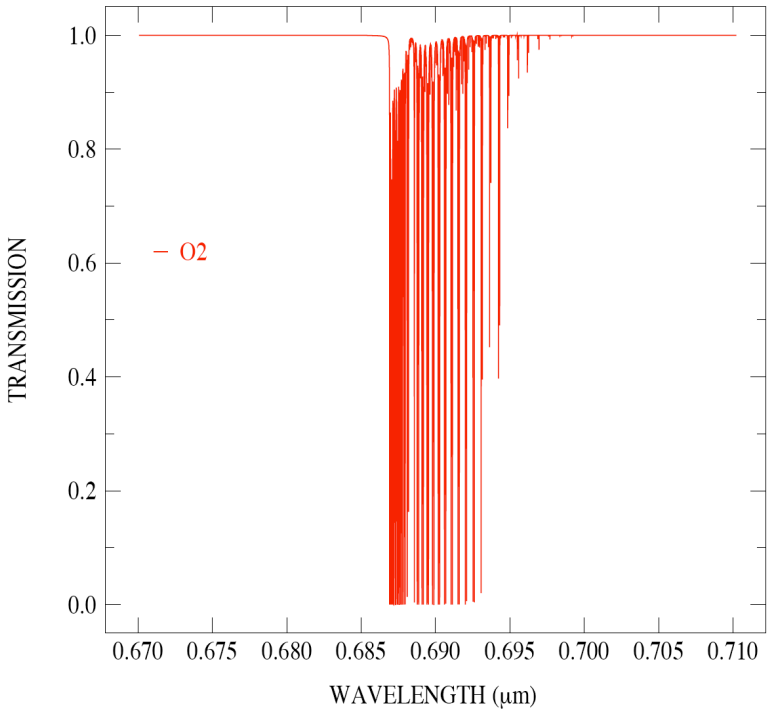

Figure 1: Spectral transmission due to oxygen absorption (B-band).

Since the two spectral bands are close wavelength-wise, we have:

$$\rho_w^{(1)} \approx \rho_w^{(2)};\ E_s^{(1)} \approx E_s^{(2)};\ T_d^{(1)}(\theta_s) \approx T_d^{(2)}(\theta_s) \tag{2}$$

L_F can be written as the product of the radiance at the peak of fluorescence emission, L_{F0}, and a spectral function, h, i.e.:

$$L_F^{(1)} = L_{F0}h^{(1)};\ L_F^{(2)} = L_{F0}h^{(2)} \tag{3}$$

Using the approximations (2) and (3) in Equations (1a) and (1b), we obtain:

$$L_{F0} = [L_0^{(1)} - L_0^{(2)} T_{O2}^{(1)}(\theta_s,P_0)]/[h^{(1)} - h^{(2)} T_{O2}^{(1)}(\theta_s,P_0)] \tag{4}$$

or, after conversion into remote sensing reflectance:

$$F_0 = [R_{RS0}^{(1)} - R_{RS0}^{(2)} T_{O2}^{(1)}(\theta_s,P_0)]/[h^{(1)} - h^{(2)} T_{O2}^{(1)}(\theta_s,P_0)] \tag{5}$$

where F_0 is the remote sensing reflectance signal at 685 nm due to fluorescence and R_{RS0} the measured remote sensing reflectance just above the surface. Thus, from measurements of R_{RS0} in the two spectral bands and knowing T_{O2} anf h, one can deduce F_0.

Measuring from space

In this case, Equations (1a) and (1b) become:

$$L_{TOA}^{(1)} = L_a^{(1)} T_{O2}^{(1)}(\theta_s,\theta_v,P_a) + \rho_w^{(1)} E_s^{(1)} cos(\theta_s) T_d^{(1)}(\theta_s)\, T_d^{(1)}(\theta_v) T_{O2}^{(1)}(\theta_s,\theta_v,P_0)/\pi + L_F^{(1)}\, T_d^{(1)}(\theta_v)\, T_{O2}^{(1)}(\theta_v,P_0) \quad (6a)$$

$$L_{TOA}^{(2)} = L_a^{(2)} + \rho_w^{(2)} E_s^{(2)} cos(\theta_s) T_d^{(2)}(\theta_s)\, T_d^{(2)}(\theta_v)/\pi + L_F^{(2)}\, T_d^{(2)}(\theta_v) \quad (6b)$$

where L_{TOA} is the top-of-atmosphere radiance, θ_v is viewing zenith angle, $T_{O2}(\theta_s,\theta_v,P_a)$ is the oxygen transmittance associated with the path radiance, $T_{O2}(\theta_s,\theta_v,P_0)$ is the oxygen transmittance associated with the elastic water reflectance (along the path sun to surface and surface to satellite), and $T_{O2}(\theta_v,P_0)$ is the oxygen transmittance associated with the fluorescence signal (only along the path surface to satellite). The transmittances $T_{O2}(\theta_s,\theta_v,P_a)$ and $T_{O2}(\theta_s,\theta_v,P_0)$ are different, the first one in particular depends significantly on the vertical distribution of the aerosols (average pressure P_a), as discussed in the next section.

Let us assume that

$$\rho_w^{(1)} \approx \rho_w^{(2)};\; E_s^{(1)} \approx E_s^{(2)}\, T_d^{(1)}(\theta) \approx T_d^{(2)}(\theta) \quad (7)$$

and

$$L_a^{(1)} \approx L_a^{(2)};\; T_{O2}^{(1)}(\theta_s,\theta_v,P_a) \approx T_{O2}^{(1)}(\theta_s,\theta_v,P_0) \quad (8)$$

Using these approximations and Equation (3), we obtain:

$$L_{F0} = [L_{TOA}^{(1)} - L_{TOA}^{(2)} T_{O2}^{(1)}(\theta_s,\theta_v,P_0)]/T_d(\theta_v)\, [h^{(1)} T_{O2}^{(1)}(\theta_v,P_0) - h^{(2)} T_{O2}^{(1)}(\theta_s,\theta_v,P_0)] \quad (9)$$

or, by transforming top-of-atmosphere radiance into reflectance, i.e., $\rho_{TOA} = \pi L_{TOA}/E_s cos(\theta_s)$:

$$F_0 = [\rho_{TOA}^{(1)} - \rho_{TOA}^{(2)} T_{O2}^{(1)}(\theta_s,\theta_v,P_0)]/\pi T_d(\theta_s) T_d(\theta_v) [h^{(1)} T_{O2}^{(1)}(\theta_v,P_0) - h^{(2)} T_{O2}^{(1)}(\theta_s,\theta_v,P_0)] \quad (10)$$

This equation is similar to Equation (5) and allows one to estimate F_0 from the top-of-atmosphere reflectance ρ_{TOA} knowing $T_{O2}(\theta_s,\theta_v,P_0)$. However, accuracy will depend on the assumptions made, in particular that $T_{O2}^{(1)}(\theta_s,\theta_v,P_a) \approx T_{O2}^{(1)}(\theta_s,\theta_v,P_0)$.

3. RADIATIVE TRANSFER MODELING AND SIMULATIONS

The top-of-atmosphere reflectance was simulated using the radiative transfer code GAME[5]. In this code, gaseous absorption is calculated at high spectral resolution, using a line-by-line code. The HITRAN 2004 database is used to define spectroscopic parameters for oxygen absorption lines. Multiple scattering effects are treated from the Adding Doubling Method[6]. In this method, the radiative transfer equation is solved assuming a vertically inhomogeneous atmosphere stratified into plane and homogeneous layers. The GAME code accounts for scattering by molecules and aerosols, absorption by aerosols, Fresnel reflection at the air-sea interface, and diffuse reflection by the water body. An accurate treatment of the roughness of the sea caused by wind is included from wave-slope probability density, to account for interactions with the atmospheric radiance field.

The elastic reflectance of the water body was modeled as a function of chlorophyll-a concentration (C, mgm^{-3}), sediment concentration (S, gm^{-3}), and yellow substance absorption at 440 nm (A_y440, m^{-1}). Typical relations and coefficients are used to describe absorption and scattering by phytoplankton and mineral particles, and absorption by dissolved substances[7, 8]. The rate of chlorophyll-a fluorescence was expressed in terms of chlorophyll-a concentration, absorption coefficient of algae, a factor accounting for intracellular re-absorption of fluorescence within the emission spectral band, the quantum yield of fluorescence, and photo-synthetically available radiation[9]. The fluorescence yield, which ranges from less than 0.01 to 0.10, was fixed at 0.05.

Using the above modeling, R_{RS0}, ρ_{TOA}, and the various atmospheric functions, i.e., oxygen transmittances and diffuse atmospheric transmittance, were simulated for applying the methodology to four sets of spectral bands, namely [686.8 - 688.3; 681.0 - 686.0], [686.8 - 687.3; 681.0 - 686.0], [686.8 - 688.3; 683.1 - 692.0], and [686.8 - 687.3; 683.1 - 691.0]. The first two sets have spectral bands in and outside the oxygen B-band, and the last two sets have spectral bands centered on the same wavelength. The spectral bands strongly affected by oxygen absorption are 0.5 or 1.5 nm wide.

The simulations were performed for a single angular geometry, i.e., a solar zenith angle of 60 degrees, a viewing zenith angle of 15 degrees, and a relative azimuth angle of 90 degrees. Surface is assumed to be flat. Aerosols are of maritime type, with optical thickness of 0.1 and 0.2. The vertical profile of aerosol concentration is exponential with scale heights of 0.25, 0.5, 1, 2, and 3 km. Surface pressure is 1013 mb. Three sets of cases are considered for the elastic water reflectance, each set with chlorophyll-a concentration of 0.1, 1, 5, and 30 mg^{-3}. The $[A_y440, S]$ values are [0, 0], [0.5 m^{-1}, 2 gm^{-3}], [2 m^{-1}, 5 gm^{-3}], respectively.

Figure 2 displays the remote sensing reflectance (just above surface) for the three sets of cases. As sediment concentration increases, the fluorescence signal is more difficult to distinguish from the background reflectance, and the baseline less easy to draw. Chlorophyll absorption near 670 nm introduces further difficulty. Figures 3 and 4 display as a function of aerosol scale height the oxygen transmittance associated with water reflectance, $T_{O2}(\theta_s,\theta_v,P_0)$, and atmospheric reflectance, $T_{O2}(\theta_s,\theta_v,P_a)$, respectively. The first transmittance (Figure 3) is fairly independent of aerosol scale height and optical thickness, whereas the second transmittance (Figure 4) depends significantly on the amount and vertical distribution of aerosols, decreasing with increasing optical thickness and increasing with increasing scale height.

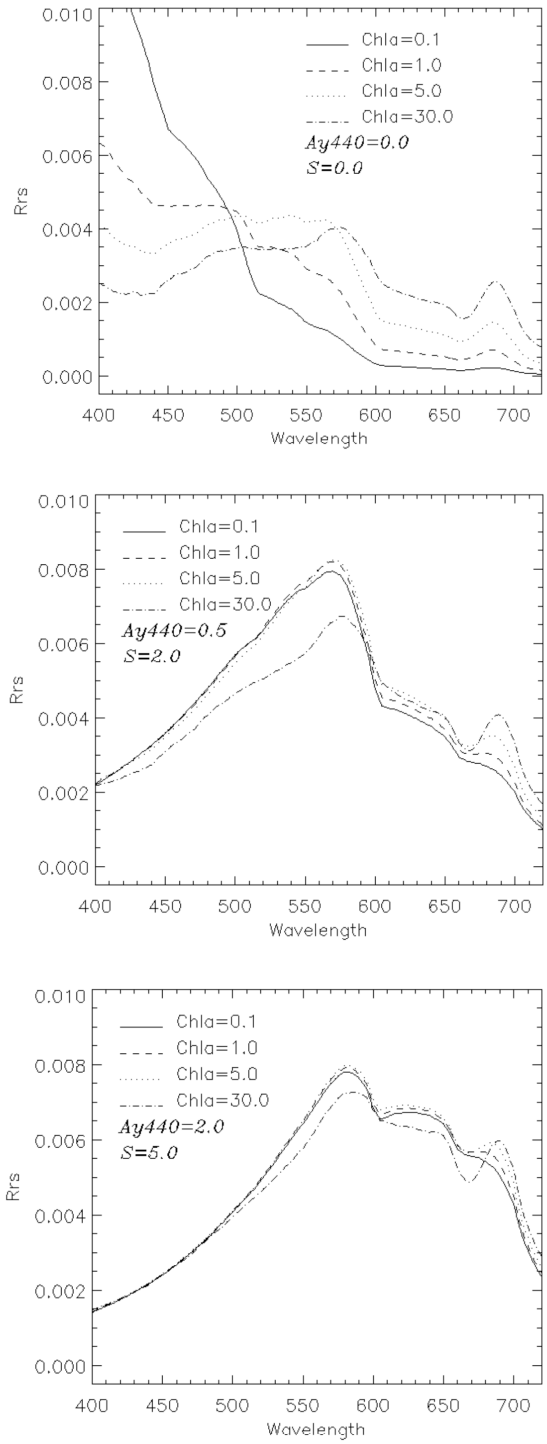

Figure 2: Remote sensing reflectance as a function of wavelength for chlorophyll concentrations of 0.1, 1, 5, and 30 mgm^{-3}. (Top) $A_y440 = 0$ and $S = 0$. (Middle) $A_y440 = 0.5\ m^{-1}$ and $S = 2\ gm^{-3}$. (Bottom) $A_y440 = 2\ m^{-1}$, and $S = 5\ gm^{-3}$.

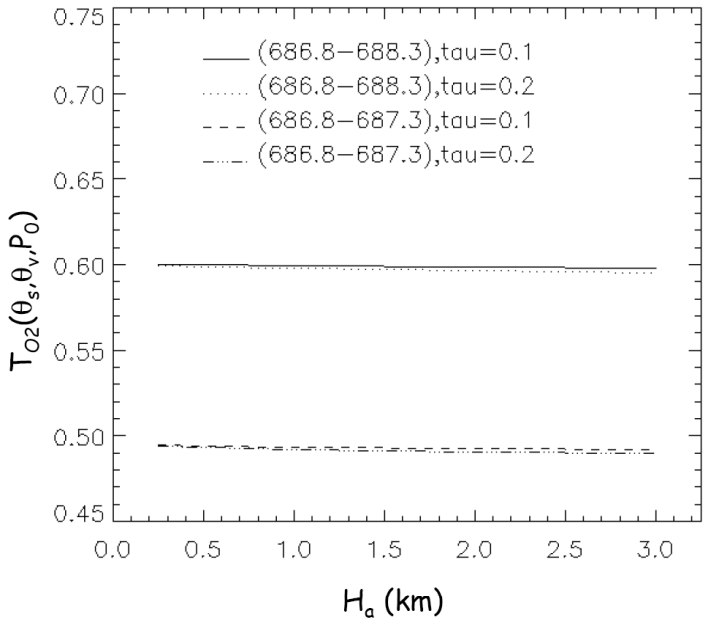

Figure 3: Oxygen transmittance associated with elastic water-leaving radiance, $T_{O2}(\theta_s,\theta_v,P_0)$, as a function of aerosol scale height, H_a, for spectral bands [686.8-688.3] and [686.8-687.3] and aerosol optical thicknesses of 0.1 and 0.2.

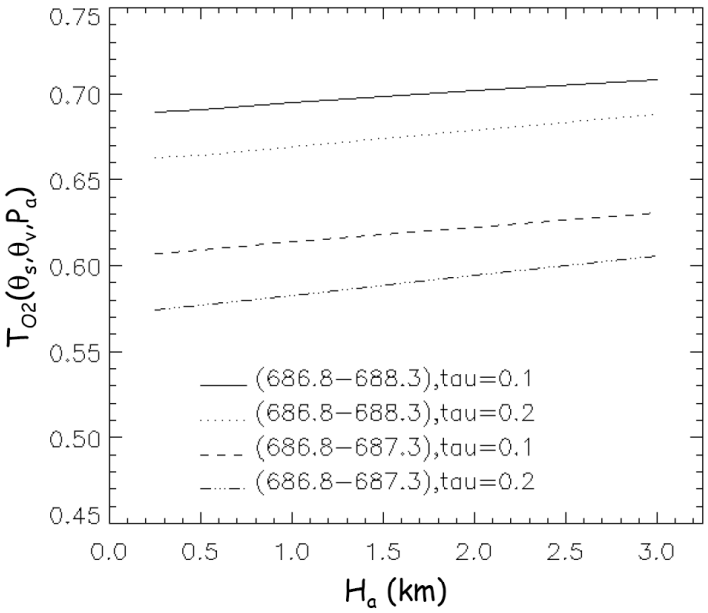

Figure 4: Oxygen transmittance associated with atmospheric path radiance, $T_{O2}(\theta_s,\theta_v,P_a)$, as a function of aerosol scale height, H_a, for spectral bands [686.8-688.3] and [686.8-687.3] and aerosol optical thicknesses of 0.1 and 0.2.

The differences between $T_{O2}(\theta_s,\theta_v,P_0)$ and $T_{O2}(\theta_s,\theta_v,P_a)$ make the approximation $T_{O2}^{(1)}(\theta_s,\theta_v,P_a) \approx T_{O2}^{(1)}(\theta_s,\theta_v,P_0)$ not well justified. The impact on fluorescence retrieval would be easily taken into account if $T_{O2}(\theta_s,\theta_v,P_a)$ were independent on aerosol amount and vertical structure, but this is not the case. Therefore applying the method from space requires knowing aerosol path radiance, optical thickness, and vertical distribution. Aerosol path radiance and optical thickness can be obtained from observations in the near infrared, where water is generally black or little reflecting, and scale height from observations in the oxygen A-band. Assuming an average aerosol vertical distribution, however, may yield reasonable results, as demonstrated in the next section.

4. RESULTS

Table 1 summarizes the performance of the methodology in the absence of radiometric noise when measurements are made just above the surface. The fluorescence signal is generally overestimated, but the influence of elastic reflectance is small with spectral bands centered on the same wavelength, resulting in F_0 errors of less than 2% for S = 0 and 2 gm^{-3} and 9% for S = 5 gm^{-3}. With non-overlapping spectral bands, the F_0 errors may reach over 300% at C = 0.1 mgm^{-3}. For a given A_y440 and S, the larger relative errors are obtained, not surprisingly, at low chlorophyll-a concentration, i.e., when the fluorescence signal is small.

Table 1: Relative error ΔF_0 (%) on F_0 for various sets of spectral bands, i.e., (1) [686.8 - 688.3; 681.0 - 686.0], (2) [686.8 - 687.3; 681.0 - 686.0], (3) [686.8 - 688.3; 683.1 - 692.0], and (4) [686.8 - 687.3; 683.1 - 691.0]. The ocean is viewed from just above the surface. No radiometric noise.

[Chl-a]	F_0	$\Delta F_0^{(1)}$	$\Delta F_0^{(2)}$	$\Delta F_0^{(3)}$	$\Delta F_0^{(4)}$
Ay(440) = 0; S = 0					
0.1	0.0029	-8.88	-4.88	0.14	0.04
1.0	0.0093	-7.08	-3.87	0.24	0.08
5.0	0.0183	-2.69	-1.44	0.49	0.18
30.0	0.0327	11.37	6.22	0.60	0.16
Ay(440) = 0.5 m^{-1}; S = 2 gm^{-3}					
0.1	0.0029	-198.92	-109.29	3.12	0.83
1.0	0.0093	-54.48	-29.83	1.72	0.59
5.0	0.0183	-11.32	-6.09	1.69	0.64
30.0	0.0327	22.16	12.12	1.22	0.32
Ay(440) = 2 m^{-1}; S = 5 gm^{-3}					
0.1	0.0029	-311.21	-170.26	8.47	3.02
1.0	0.0093	-80.04	-43.61	3.72	1.42
5.0	0.0183	-12.51	-6.60	2.91	1.13
30.0	0.0327	34.57	18.92	1.83	0.49

(ΔF_0 in %.)

The effect of radiometric noise on retrieval accuracy is significant, and for some noise levels may completely dominate the effect of elastic water reflectance. This is shown in Table 2, which gives for $A_y440 = 2$ m^{-1} and S = 5 gm^{-2} the F_0 error due to a white radiometric noise of 0.00001 and 0.0001 on R_{RS0}. For the two sets of spectral bands centered on the same wavelength, the inaccuracy introduced by a noise of 0.00001 is about ±2% at C = 30 mgm^{-3}, becoming ±25 and ±20% with a noise of 0.00001. Thus, a noise of only a few 0.00001 is acceptable to yield adequate fluorescence estimates, and this will be easier to achieve for the [686.8-688.3] nm band (1.5 nm wide) than for the [686.8-687.3] nm band (0.5 nm wide). Figure 5 compares the actual and retrieved fluorescence signal in the presence of a radiometric noise of 0.00001 when the sediment load is large (5 gm^{-3}). Even though the total remote sensing reflectance is dominated by the elastic water reflectance, the fluorescence information is extracted with good accuracy.

Table 2: Effect of radiometric noise on the retrieval of F_0 for various sets of spectral bands, i.e., (1) [686.8 - 688.3; 681.0 - 686.0], (2) [686.8 - 687.3; 681.0 - 686.0], (3) [686.8 - 688.3; 683.1 - 692.0], and (4) [686.8 - 687.3; 683.1 - 691.0]. The ocean is viewed from just above the surface.

[Chl-a]	F_0	$\Delta F_0^{(1)}$	$\Delta F_0^{(2)}$	$\Delta F_0^{(3)}$	$\Delta F_0^{(4)}$
0.00001 noise					
0.1	0.0029	34.66	24.69	27.82	21.08
1.0	0.0093	11.02	7.85	8.85	6.70
5.0	0.0183	5.58	3.98	4.48	3.40
30.0	0.0327	3.12	2.22	2.50	1.90
0.0001 noise					
0.1	0.0029	346.58	246.90	278.22	210.80
1.0	0.0093	110.21	78.51	88.47	67.03
5.0	0.0183	55.83	39.78	44.82	33.96
30.0	0.0327	31.24	22.25	25.08	19.00

(ΔF_0 in %.)

Accuracy is degraded when the measurements are made from space, as shown in Table 3, which is directly comparable to Table 1 for the case of measuring from just above the surface. This is chiefly due to the dependence of $T_{O2}(\theta_s,\theta_v,P_a)$ on aerosol vertical profile, which in Table 3 is unknown and assumed to be exponential with a scale height of 1 km, but is actually exponential with a scale height of 0.5 km. In this situation, F_0 is mostly underestimated when using spectral bands centered on the same wavelength, with relative errors of -80 to -100% at $C = 0.1$ mgm^{-3} and -5 to -8% at $C = 30$ mgm^{-3}. Compared with the standard baseline technique used for MERIS, however, the gain in accuracy is substantial (Table 4). With the set of spectral bands [686.8 - 688.3; 683.1 - 692.0] nm, and for the case of $A_y440 = 2$ m^{-1} and $S = 5$ gm^{-2}, the relative F_0 error is reduced from about -460% to -80% at $C = 0.1$ mg^{-3} and from -19% to -5% at $C = 30$ mgm^{-3}. Note that in the case of the standard baseline technique the atmospheric correction is assumed to be perfect, and in the case of the differential absorption technique the aerosol optical thickness and the atmospheric path radiance are supposedly known. Of course, retrieval accuracy using the oxygen B-band methodology would be further degraded if the actual aerosol structure were more different from the assumed structure.

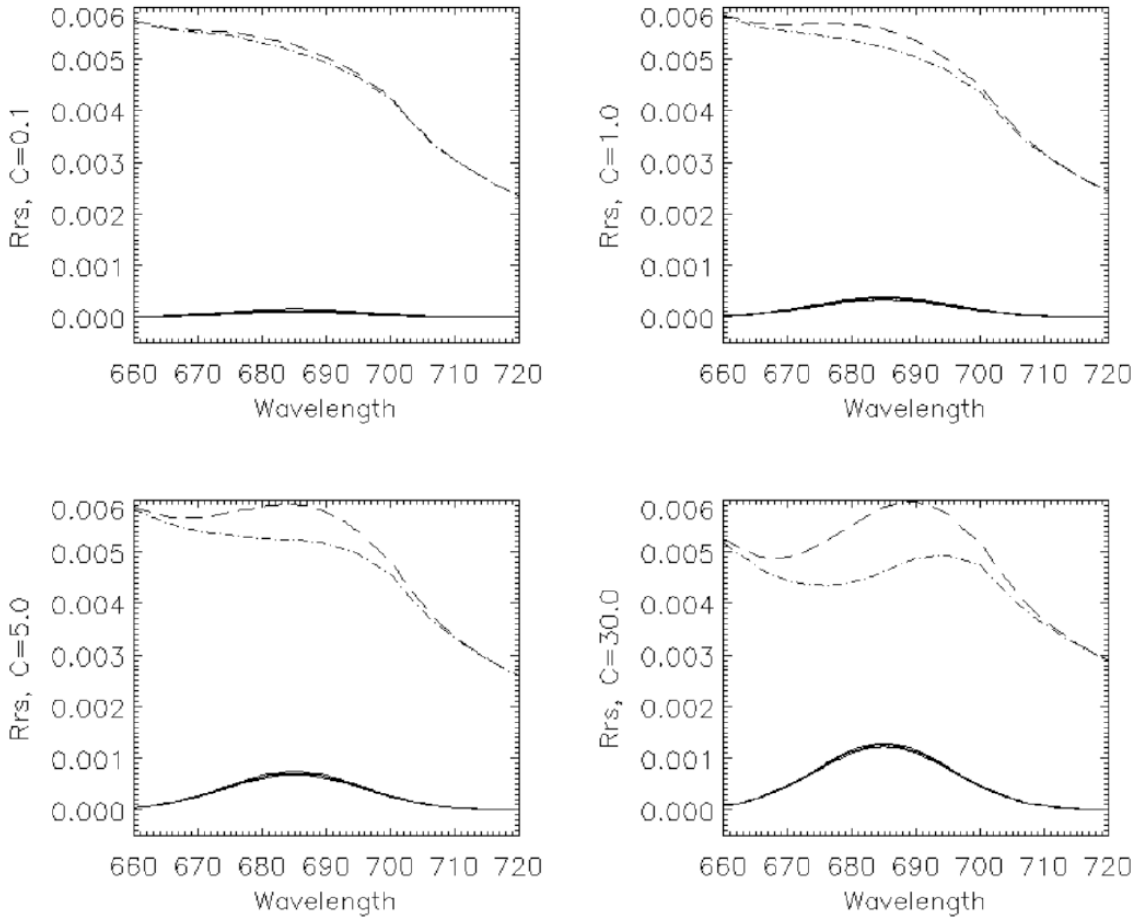

Figure 5: Retrieved fluorescence signal from measurements just above the surface in spectral bands [686.8 - 688.3] and [683.1 - 692.0]. A_y440 = 2 m^{-1}; S = 5 gm^{-3}. Radiometric noise is 0.00001. Dashed line is total reflectance, dash-dotted line is elastic reflectance, dotted line is the fluorescence signal, and the solid lines delineate the error on the fluorescence estimates.

5. CONCLUSIONS

The differential absorption method using the oxygen B-band works well when viewing the ocean from just above the surface, in both Case I and Case II waters, even with high sediment levels. Pairs of spectral bands centered on the same wavelength provide the best results, with a small loss of sensitivity. No assumptions or information about the atmosphere and surface are required. In the presence of typical radiometric noise, expected accuracy on fluorescence retrievals is <10% for chlorophyll concentrations above 1 mgm^{-3} when using spectral bands centered on the same wavelength. This constitutes the basis for a new field technique to measure chlorophyll fluorescence that can be used in satellite retrieval evaluation and eco-physiological studies.

Table 3: Relative error ΔF_0 (%) on F_0 for various sets of spectral bands, i.e., (1) [686.8 - 688.3; 681.0 - 686.0], (2) [686.8 - 687.3; 681.0 - 686.0], (3) [686.8 - 688.3; 683.1 - 692.0], and (4) [686.8 - 687.3; 683.1 - 691.0]. The ocean is viewed from space. No radiometric noise. The aerosol scale height, H_a, is assumed to be 1 km in the retrieval algorithm, but it is actually 0.5 km.

[Chl-a]	F_0	$\Delta F_0^{(1)}$	$\Delta F_0^{(2)}$	$\Delta F_0^{(3)}$	$\Delta F_0^{(4)}$
Ay(440) = 0; S = 0					
0.1	0.0029	-126.63	-108.34	-98.81	-95.96
1.0	0.0093	-45.36	-37.19	-31.05	-30.39
5.0	0.0183	-21.91	-18.23	-15.05	-15.15
30.0	0.0327	3.16	-1.89	-7.80	-8.38
Ay(440) = 0.5 m^{-1}; S = 2 gm^{-3}					
0.1	0.0029	-354.09	-231.80	-93.19	-94.57
1.0	0.0093	-102.09	-67.88	-28.26	-29.49
5.0	0.0183	-32.24	-23.73	-12.79	-14.36
30.0	0.0327	16.06	5.08	-6.63	-8.09
Ay(440) = 2 m^{-1}; S = 5 gm^{-3}					
0.1	0.0029	-488.48	-303.89	-83.10	-90.74
1.0	0.0093	-132.69	-84.18	-24.50	-28.05
5.0	0.0183	-33.66	-24.33	-10.47	-13.50
30.0	0.0327	30.92	13.13	-5.49	-7.79

(ΔF_0 in %; Actual H_a = 0.5 km; Assumed H_a = 1 km.)

Table 4: Comparison of the differential absorption method using spectral bands [686.8-688.3] and [683.1-692.0] with the standard MERIS baseline technique. The ocean is characterized by $A_y 440$ = 2 m^{-1} and S = 5 gm^{-3}. No radiometric noise.

Ay(440) = 2 m^{-1}; S = 5 gm^{-3}

[Chl-a]	F_0	ΔF_0(O_2 B-Band)*	ΔF_0(MERIS)
0.1	0.0029	-83.10	461.53
1.0	0.0093	-24.50	124.33
5.0	0.0183	-10.47	37.36
30.0	0.0327	-5.49	-19.25

(ΔF_0 in %.)

*[686.8 - 688.3; 683.1 - 692.0]

Accuracy is degraded when viewing the ocean from space, due to differences between $T_{O2}(\theta_s,\theta_v,P_0)$ and $T_{O2}(\theta_s,\theta_v,P_a)$, and the dependence of $T_{O2}(\theta_s,\theta_v,P_a)$ on aerosol vertical structure. In this case, knowledge of aerosol path radiance and aerosol optical thickness is required. Assuming an average aerosol vertical distribution, however, yields reasonable results. Accuracy is increased when θ_s is larger and θ_v is lower, because the difference between the oxygen transmittance associated with the elastic water reflectance and with the fluorescence signal is larger (more sensitivity). In comparison with the standard baseline technique, substantial improvements in retrieval accuracy are expected in Case II waters, especially in the presence of sediments. This is significant in view of the information chlorophyll fluorescence can provide, not only on chlorophyll concentration, but also on photosynthetic activity and quantum yield, whose variability may be linked to differences in phytoplankton species, nutrient supply, and light availability. The methodology can be tested with Envisat's SCHIAMACHY, which measures between 604 and 905 nm at a spectral resolution of 0.48 nm.

ACKNOWLEDGMENTS

This work was supported by grants from the National Aeronautics and Space Administration and the Scripps Institution of Oceanography. The programming support of Mr. John McPherson, Scripps Institution of Oceanography, is gratefully acknowledged.

REFERENCES

1. R. A. Neuville and J. F. R. Gower, 'Passive remote sensing of phytoplankton via chlorophyll-a fluorescence', *J. Geophys. Res.*, 82, 3487-3493, 1977.
2. Y. Huot, C. A. Brown, and J. J. Cullen, 'New algorithms for MODIS sun-induced chlorophyll fluorescence and a comparison with present data products', *Limnol. Oceanogr.: Methods*, 3, 108-130, 2005.
3. R. Letelier and M. R. Abbott, 'An analysis of chlorophyll fluorescence algorithms for the Moderate Resolution Imaging Spectrometer (MODIS)', *Remote Sen. Environ.*, 58, 215-223.
4. J. F. R. Gower, R. Doerffer, and G. A. Borstad, 'Interpretation of the 685 nm peak in water-leaving radiance spectra in terms of fluorescence, absorption and scattering, and its observation by MERIS', *Int. J. Remote Sensing*, 20, 1771-1786, 1999.
5. P. Dubuisson, J. C. Buriez, and Y. Fouquart, 'High Spectral Resolution Solar Radiative Transfer in Absorbing and Scattering media, application to the satellite simulation', *J. Quant. Radiat. Transfer*, 55, 103-126, 1996.
6. J. F. De Haan, P. B. Bosma, and J. W. Hovenier, 'The adding method for multiple scattering calculations of polarized light', *Astronom. Astrophys.*, 183, 371, 1987.
7. A. Morel and S. Maritorena, 'Bio-optical properties of oceanic waters: A reappraisal', *J. Geophys. Res.*, 106, 7163-7180, 2002.
8. S. Tassan, 'Local algorithms using SeaWiFS data for the retrieval of phytoplankton, pigments, suspended sediment, and yellow substance in coastal waters', *Appl. Opt.*, 23, 2369-2378, 1994.
9. M. Babin, A. Morel, and B. Gentilli, 'Remote sensing of sea surface Sun-induced clorophyll fluorescence: Consequences of natural variations in the optical characteristics of phytoplankton and the quantum yield of chlorophyll-a fluorescence', *Int. J. Remote Sensing*, 17, 2417-2448, 1996.